A LTE-BASED WIDEBAND DISTRIBUTED SPECTRUM SHARING ARCHITECTURE

Mingming Cai (mcai@nd.edu)[1] and J. Nicholas Laneman (jnl@nd.edu)[1]

[1]University of Notre Dame, Notre Dame, IN, 46556, USA

ABSTRACT

This paper describes a radio architecture for distributed spectrum sharing among secondary users (SUs) in a localized area and a wide band of frequencies. Based upon an orthogonal frequency-division multiplexing (OFDM) physical layer, the architecture allows multiple pairs of SUs to utilize one or more sub-channels within the band without causing harmful interference to each other. The spectrum utilized by a SU pair may be contiguous or discontiguous; it can be changed dynamically based upon spectrum sensing at the transmitter, and the receiver tracks transmission using synchronization and control messages from the transmitter. A prototype implementation of the architecture has been developed using National Instruments hardware and software, specifically USRP RIOs as well as the LabVIEW Communications System Design Suite (CSDS) and associated LTE Application Framework, respectively. System tests show that the spectrum sharing efficiency of the implemented distributed spectrum sharing system is close to an upper bound when signal-to-noise ratio (SNR) is high enough. We also identify the imaged interference caused by hardware IQ imbalance as the main source of interference.

1. INTRODUCTION

In 2015, the global mobile data traffic grew 74 percent while the mobile network connection speed only grew 20 percent. The mobile traffic will continue growing 53 percent annually over the next five years [1]. The astonishing growth of wireless technologies and the number of wireless devices have led to a significant amount of spectrum demands. Easier access to spectrum plays an important role in economic growth and technological leadership [2].

There are two basic directions to exploit more spectrum resources, reusing current under-utilized bands through cognitive radio (CR) and dynamic spectrum access (DSA) and exploring spectrum opportunities in higher frequency, i.e., millimeter wave bands. However, signal in millimeter experiences much higher path loss than that of signal below 6 GHz [3]. Sharing under-utilized spectrum has advantages over the millimeter wave communication, such as high coverage range and low cost. The spectrum could be shared across time, frequency, and space [4], [5].

To accelerate industry, academia and government correlations to develop technologies and policies for better spectrum utilization in the US, National Spectrum Consortium has been formed [6]. The Federal Communications Commission (FCC) has also announced a new Citizens Broadband Radio Service (CBRS) in the 3550-3700 MHz Radar Band for shared wireless broadband [7].

PCAST and FCC recommend that the shared spectrum be classified into three tiers [2, 7]. The first tier is the legacy or incumbent federal users, which would be granted full protections for the operations within deployed areas. The second tier consists of users with short-term priority authorizations to operate in designated spectrum and geographic areas. Second tier users receive protection from interference of the third tier users, but are subject to the interference from the first tier users. The third tier user could only utilize the spectrum on an opportunistic basis, and no interference protection is provided. The first and second tier users correspond to primary users (PUs), and the third tier users correspond to secondary users in the traditional DSA context.

There are two key issues that need to be addressed, spectrum opportunities identification and spectrum resources assignment for SUs [8]. Databases and spectrum sensing are key approaches for spectrum opportunities identification. Database can assist spectrum opportunities identification by directly providing PUs' spectrum usage information and by improving the quality of spectrum sensing with detailed signaling parameters and prior information, such as PU power levels, locations and dwell times [9]. Energy detection, matched filter detection and feature detection are typical methods for single-band spectrum sensing [10]. Wideband spectrum sensing algorithms are also proposed to allow opportunistic access in wideband spectrum.

A channel assignment protocol is required to allocate spectrum resources and to coordinate SUs for coexistence with the PUs as well as with each other. Channel assignment is typically a key feature of the Medium Access Control (MAC) protocol. A large number of MAC protocols have been developed for spectrum sharing systems e.g. [8, 11–14].

In this paper, we develop a radio architecture for distributed spectrum sharing. The architecture includes a database, wideband spectrum sensing, a channel assignment protocol, and a flexible physical layer. We analyze the requirements of the four system components. Based on the requirements, a flexible physical layer is developed and validated to support distributed spectrum sharing [15]. We also design and implement the wideband spectrum sensing and the channel assignment protocol. The wideband spectrum sensing component, channel assignment protocol and flexible physical layer are integrated together,

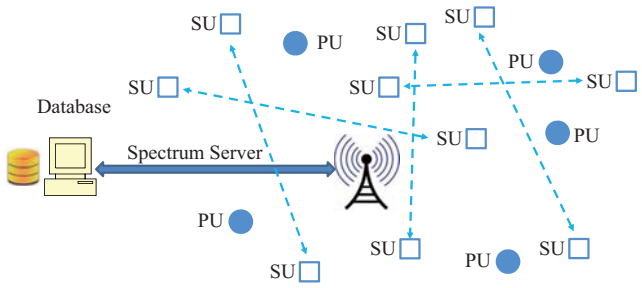

Figure 1: Scenario considered.

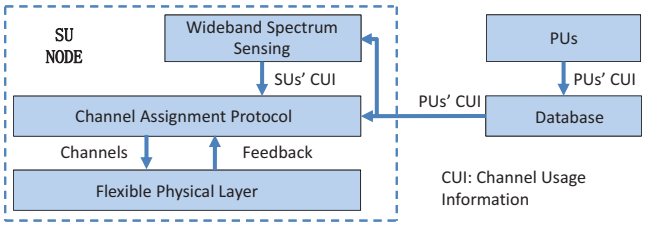

Figure 2: The architecture of the wideband spectrum sharing system. The database provides PUs' channel usage information (CUI), and the wideband spectrum sensing provides SUs' CUI.

and the whole system is validated with USRP RIOs as well as the LabVIEW Communications System Design Suite (CSDS) [16].

2. SYSTEM ARCHITECTURE

We consider a local area with PUs and SUs, and candidates of shared spectrum as shown in Figure 1. A spectrum access system (SAS), consisting of spectrum server and database, protects PUs from interference of SUs. SAS can either eliminate certain frequency and time slots from SUs' consideration or provides potential frequency and time slots available to SUs through periodic broadcast messages. Each SU uses distributed wideband spectrum sensing and channel assignment protocol to share the spectrum.

Our goal is to develop an elaborate and evolvable architecture for distributed system sharing that enables experimental validation over the air with dozens of nodes.

As shown in Figure 2, our system architecture for wideband spectrum sharing has four components, i.e., database, wideband spectrum sensing, channel assignment protocol, and flexible physical layer. Database and wideband spectrum sensing assist channel opportunities identification. Specifically, database provides PUs' channel usage information (CUI), and wideband spectrum sensing helps to identify the channel usage of other SUs. Channel assignment is achieved by channel assignment protocol, and the flexible physical layer is designed to meet the requirements of the channel assignment protocol.

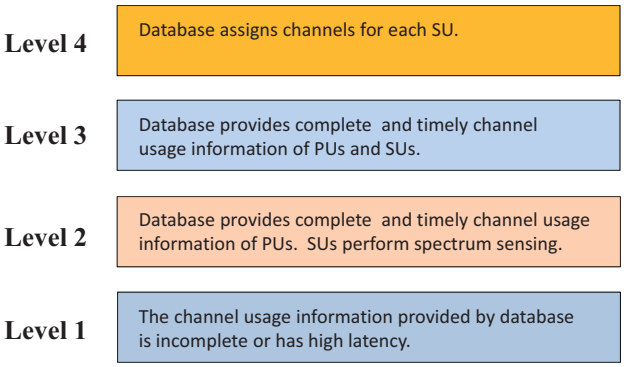

Figure 3: Database levels.

2.1. Database

As discussed in [8], a database can provide four levels of information. Figure 3 illustrates the four levels. As the database level goes up, the database provides more information to the SUs, but the requirements and overhead for the database also increase.

PUs usually have more stringent interference requirements than SUs. SUs need timely CUI of other SUs. As a result, we focus on the second-level database to provide good protection for the PUs. SUs could obtain correct and timely PUs' CUI from the database. SUs conduct wideband spectrum to obtain other SUs' CUI. PUs are sparse, but the SUs are likely not.

Two communication links are required, namely, database-SUs link and database-PUs link. Generally, one-way mode, broadcasting PUs CUI to the SUs, is sufficient to database-SUs link. Database-PUs link could be either one-way or two-way, depending on the link reliability requirements.

2.2. Wideband Spectrum Sensing

Wideband spectrum sensing algorithms includes Nyquist sampling wideband spectrum sensing and sub-Nyquist sampling wideband spectrum sensing [5]. Examples of Nyquist sampling wideband spectrum sensing include Partial-Band Nyquist Sampling, Sequential Narrowband Nyquist Sampling. OFDM-based spectrum sensing could be applied hardware's sampling rate is high enough to cover the spectrum [17]. One example of sub-Nyquist sampling wideband spectrum sensing is Integer Undersampling. Sub-Nyquist sampling method could lead to missing spectrum opportunities if there is large number of SUs.

The wideband spectrum sensing algorithm needs to be fast, and accurate, and it is required to have low probability of false alarm and miss detection.

We design, implement and test an OFDM-based spectrum analyzer with energy detection to execute spectrum sensing for SUs' CUI.

2.3. Channel Assignment Protocol

We consider the situation of N contiguous frequency channels, labeled as $1, 2, 3..., N$. The channel bandwidth depends on multiple factors, such as total bandwidth of available spectrum and number of SUs. In our implemented physical layer, the channel bandwidth is 2 MHz.

The channel assignment protocol run on each SU is required to determine the channel for data transmission without prior coordination. Multichannel carrier sense multiple access (CSMA) has been validated to be a good channel assignment protocol to meet this requirement [14]. In this paper, Multichannel CSMA is adopted to demonstrate the architecture of wideband distributed spectrum sharing.

Multichannel CSMA assumes no matter which channel the transmitter uses, the corresponding receiver is always listening to that channel, imposing higher requirements for the physical layer.

2.4. Flexible Physical Layer

One SU pair (transmitter and receiver) is required to find each other in one of the available channels, which is called *rendezvous* [18]. In traditional rendezvous protocols, a transmitter and a receiver do frequency hopping among the N channels or among available channels according to some channel sequences and hope they could rendezvous in one of the channels [19,20]. Usually, multiple slots are needed for two nodes to rendezvous even without any interference from other radios. It would take much longer for multiple SU pairs to rendezvous if interference among SUs is considered.

The flexible physical layer should meet the following requirements:

1. **Frequency Agile**. Transmitters can utilize any subset of the N channels. Multiple transmitters can share channels through channel assignment protocol.
2. **Fast Rendezvous**. Each receiver monitors all channels for sync signal of its corresponding transmitter, and passes transmitter's control information on rendezvous channel for further demodulation and decoding. Other transmitters' signal would be ignored by the receiver.
3. **Standard-relevant Waveforms**. It assists fast implementation with better quality of service.

We now give a brief overview of our implementation of a flexible physical layer.

We adopt National Instruments (NI) USRP RIO 2953R and NI LabVIEW CSDS as hardware and software tools for physical layer prototyping, respectively. The powerful DSP-focused Xilinx Kintex-7 FPGA in USRP RIO allows time-consuming operations that are not efficient in general purpose processor.

NI provides LTE Application Framework (AF) 1.0 for SDR that implements a 3GPP-LTE release 10 compliant Time Division Duplex (TDD) downlink transmitter and receiver [21]. The

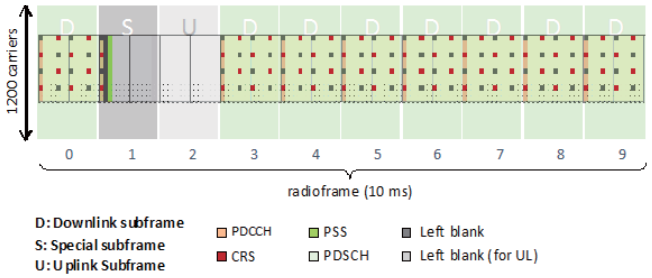

Figure 4: The resource grid of a LTE frame [21].

LTE AP is a good candidate for physical layer prototyping because of the flexible time-frequency Physical Resource Block (PRB) as shown in Figure 4.

In the LTE AF, 1200 out of 2048 OFDM subcarriers are utilized to achieve 20 MHz bandwidth. Every 12 adjacent subcarrier form a PRB. Each PRB can be individually turned on or off. The 1200 subcarriers are divided into 100 PRBs. In time domain, data is transmitted in radio frames. Every radio frame has 10 subframes, each with 14 OFDM symbols [22]. The frequency-time PRBs could be allocated to different users.

NI LTE AF is modified for our distributed spectrum sharing. In the following sections, modified AF is used to represent our modified radio based on NI LTE AF 1.0.

100 PRBs are evenly divided in to 10 PRB groups (PRBGs), and each serves as a channel. Label the 10 PRBGs as PRBG $1, 2, \ldots, 10$. The first 9 PRGs in a GRBG is for data transmission, and the left one is for guard band. Each SU pair could access any subset of the 10 channels while meeting the requirements. On the Rx side, the receiver runs 10 parallel synchronization blocks, each detecting the synchronization signal of one PRBG. In LTE, frequency-domain Primary Synchronization Signal (PSS) is used for synchronization as well as cell ID. Mobile station could identify which cell the signal comes from based on PSS. In the modified AF, different SU pairs use different PSS to distinguish each other. In the LTE AF, PDCCH and CRS are across 100 PRBs in frequency domain even PRBs are not used for data. To eliminate the interference of the PDCCH and CRS to other SUs, PDCCH is squeezed into the PRBG where PSS is transmitted, and CRS is only transmitted where there is data.

The flexible physical layer has been implemented and validated in [15]. Test in [15] demonstrates that the modified AF is fairly robust to the out-of-band interfere. However, the SNR required for full data success rate is as high as 17 dB. The main reason is that the added Low Pass Filter in the synchronization loop decreases the signal power for autocorrelation.

3. SPECTRUM ANALYZER

Among the spectrum sensing methods, energy detection does not require signal's prior knowledge. An OFDM-based spectrum analyzer is developed for wideband spectrum sensing with

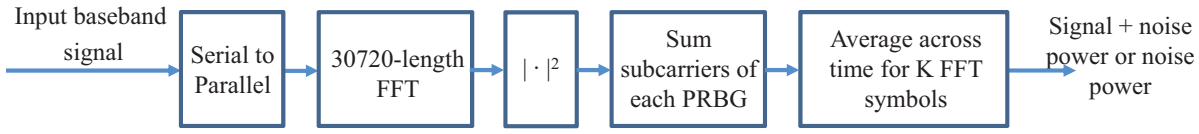

Figure 5: Signal preprocessing for the spectrum analyzer.

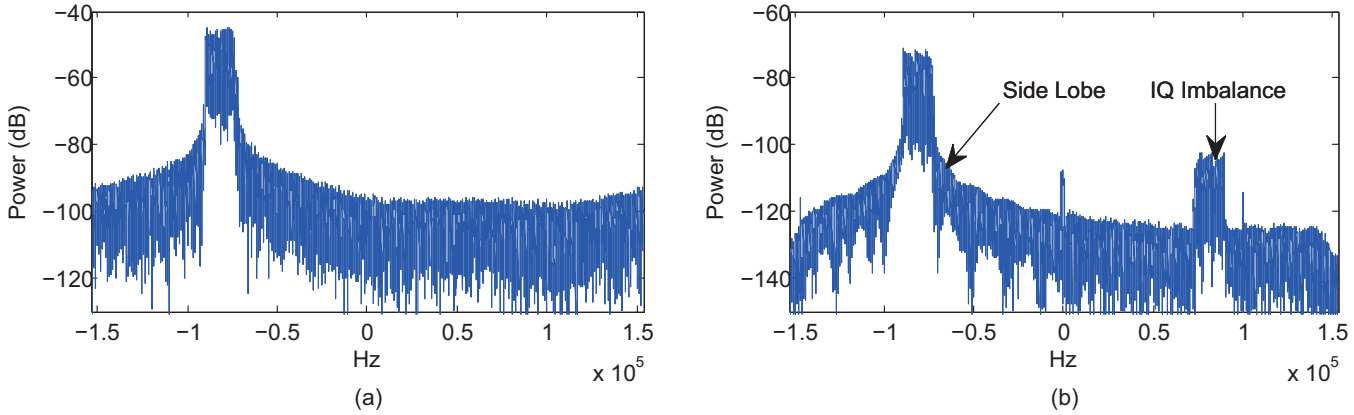

Figure 6: An example of side lobe and IQ imbalance measured from USRP. One PRBG is used for data transmission. (a) is the transmitted signal (b) is the received signal.

USRP RIO and NI CSDS.

The signal preprocessing is illustrated in Figure 5. Four steps are taken to preprocess the received data. First, 30720-length Fast Fourier Transform (FFT) is calculated to convert the time domain signal to frequency domain. 30720 is the number of samples of a LTE subframe, including Cyclic Prefix. The signal preprocessing is conducted in generator purpose processor. FFT size of 30720 is selected to save computational resource. Let $x_{i,k},\ i = 1, 2, \ldots, 30720$ be the received frequency samples after FFT and $w_{i,k},\ i = 1, 2, \ldots, 30720$ be the noise power, where $k = 1, 2, \ldots, K$ denotes index of FFT symbol. Second, calculate power of each frequency samples $|x_{i,k}|^2$. Third, sum all the frequency samples within a PRBG for each PRBG. Fourth, average the power of each PRBG across time for K FFT symbols.

The output of the signal preprocessing block for PRBG n would be

$$y_n = \frac{1}{K}\sum_{k=1}^{K}\sum_{i\in\mathcal{D}_j}|x_{i,k}+w_{i,k}|^2, n = 1, 2, \ldots, N, \quad (1)$$

where N is the number of PRBGs and $\mathcal{D}_n$ is the set of FFT samples belonging to PRBG n. Each PRBG can be detected separately. For PRBG n, the hypotheses would be

$$\mathcal{H}_{0,n}: y_n = \frac{1}{K}\sum_{k=1}^{K}\sum_{i\in\mathcal{D}_j}|w_{i,k}|^2, \quad (2)$$

$$\mathcal{H}_{1,n}: y_n = \frac{1}{K}\sum_{k=1}^{K}\sum_{i\in\mathcal{D}_j}|x_{i,k}+w_{i,k}|^2. \quad (3)$$

Denote probability of detection, probability of false alarm and probability of miss detection for PRBG n as $P_{D,n}$, $P_{F,n}$ and $P_{M,n}$, respectively. Then

$$P_{D,n} = \Pr\left(y_n > \lambda|\mathcal{H}_{1,n}\right), \quad (4)$$

$$P_{F,n} = \Pr\left(y_n > \lambda|\mathcal{H}_{0,n}\right), \quad (5)$$

$$P_{M,n} = \Pr\left(y_n \leq \lambda|\mathcal{H}_{1,n}\right) = 1 - P_{D,n}, \quad (6)$$

where λ is the threshold for detection. For fixed SNR, as λ increases, $P_{M,n}$ increases while $P_{D,n}$ and $P_{F,n}$ decrease. In distributed spectrum sharing system, miss detection usually has higher cost than false alarm. Therefore, λ should be chosen to be relatively small. As SNR increases, $P_{F,n}$ and $P_{M,n}$ decrease while $P_{D,n}$ increases with properly chosen λ.

In practice, the signals that cause false alarm also include signal of side lobe and signal from in-phase (I) and quadrature-phase (Q) imbalance. Usually, the side lobe adjacent to the signal in frequency domain has the highest gain. For intermediate frequency reception, IQ imbalance causes the well-known image problem as shown in Figure 6 [23]. Define the signal from

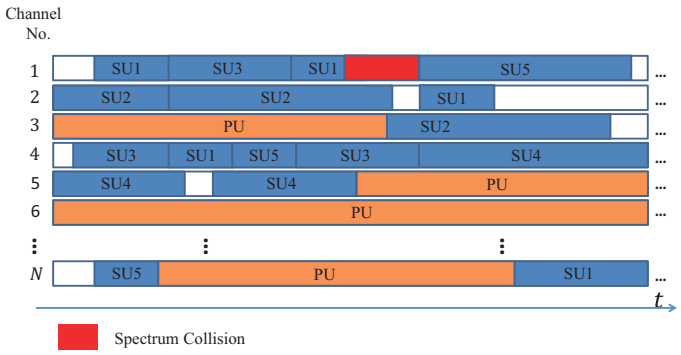

Figure 7: An example of Multichannel CSMA. The spectrum collision happens because SU5 has a miss detection error.

IQ imbalance as IQ imbalance signal. It varies with different USRPs.

In this paper, we focus on demonstration of the whole architecture. We assume SNR is high, such as more than 20 dB, to guarantee data success rate. In this case, there is more room to choose threshold so that $P_{F,n}$ and $P_{M,n}$ are small.

4. CHANNEL ASSIGNMENT PROTOCOL: MULTICHANNEL CSMA

Assume each SU has knowledge of the available channels from the database. The Multichannel CSMA Algorithm for any SU to access available channels is described in Algorithm 1.

Algorithm 1 Multichannel CSMA

1: **procedure**
2: check data arrival
3: **if** there is no data arrived **then**
4: Go to Step 2
5: **end if**
6: do wideband spectrum sensing for T_s on Tx side
7: **if** there is no available channel **then**
8: wait a random backoff time T_b
9: go to Step 6.
10: **end if**
11: randomly choose one of the available channels
12: transmit data for T_d
13: go to Step 2
14: **end procedure**

Figure 7 shows an example of the Multichannel CSMA.

4.1. Performance Metric: Spectrum Sharing Efficiency

Assume M is the number of SUs, and N is the number of available channels. Let the actual average data rate for SU m be

$$G_m = \lim_{t\to\infty} \frac{D_m(t)}{t},\ m = 1, 2, \ldots, M, \tag{7}$$

where D_m is the amount of data successfully transmitted by SU m in time t. The total actual average data rate for M users is

$$G = \sum_{m=1}^{M} G_m = \lim_{t\to\infty} \frac{\sum_{m=1}^{M} D_m}{t}. \tag{8}$$

Define performance metric, spectrum sharing efficiency as

$$E = \frac{G}{\sum_{m=1}^{M} R_m} = \lim_{t\to\infty} \frac{\sum_{m=1}^{M} D_m}{t\sum_{m=1}^{M} R_m}, \tag{9}$$

where R_m is the data rate of SU m for transmission, i.e. the data rate received if no error occurs.

4.2. Qualitative Analysis

Define collision as the event when two or more SUs transmit on the same channel at the same time.

When the database is assumed to be perfect, the overall spectrum sharing efficiency depends on three components, physical layer, spectrum sensing and channel assignment protocol. Any imperfectness of the three components could degrade system performance.

Defective physical layer causes lower data rate than expected. Signal distortion in hardware, such as IQ imbalance, nonlinearity and quantization noise, could degrade the physical layer performance. If spectrum sensing has high probability of false alarm or miss detection, the system would waste spectrum opportunities or have large number of collisions. Inefficient channel assignment protocol reduces spectrum opportunities available to SUs. Even in the case of low probability of false alarm and miss detection for spectrum sensing, collision could also happen when two or more users do spectrum sensing simultaneously and then decide to transmit on the same channel.

4.3. Upper Bound of Spectrum Sharing Efficiency

The upper bound of E could be obtained when the three system components are perfect, that is, physical layer has full data rate, and $P_{F,n} = P_{M,n} = 0,\ n = 1, 2, \ldots, N$ for all M SUs without collision.

$$\begin{aligned} E &\le \begin{cases} \dfrac{\mathbb{E}[T_d]}{T_s + \mathbb{E}[T_d]}, & M \le N \\ \dfrac{N\mathbb{E}[T_d]}{M(T_s + \mathbb{E}[T_d])}, & M > N \end{cases} \\ &= \min\left(1, \frac{N}{M}\right) \frac{\mathbb{E}[T_d]}{T_s + \mathbb{E}[T_d]}, \end{aligned} \tag{10}$$

where $\mathbb{E}[T_d]$ is the expectation of T_d.

Decreasing T_s could increase the upper bound of the spectrum sharing efficiency. However, it could also increase the probability of false alarm and miss detection. False alarm could decrease

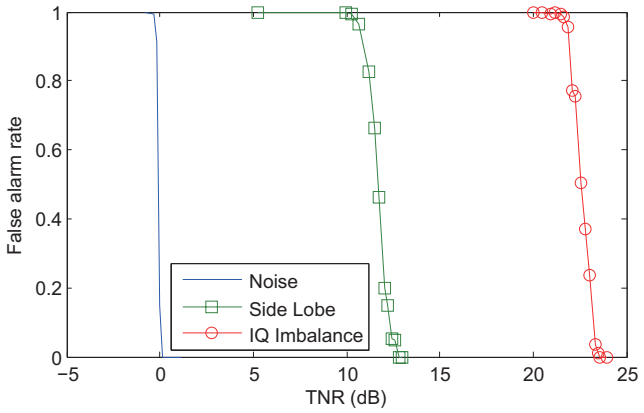

Figure 8: The false alarm rate for noise, largest side lobe signal and IQ signal imbalance as a function of threshold-to-noise ratio (TNR). The test is conducted on the USRP with the worst IQ imbalance performance. $K = 10$.

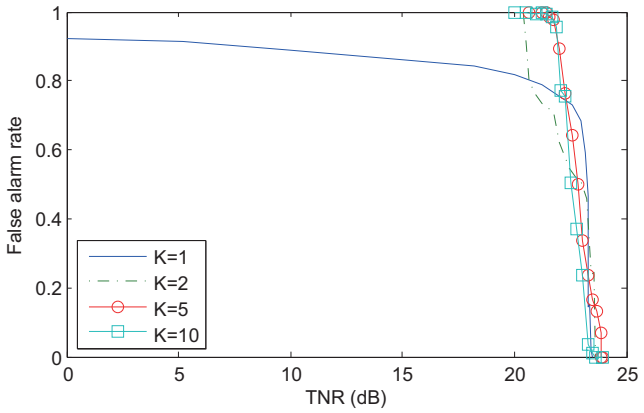

Figure 9: The false alarm rate of IQ imbalance signal as a function of TNR. The test is conducted on the USRP with the worst IQ imbalance performance. $K = 1, 2, 5, 10$.

the spectrum sharing efficiency because SU may be waiting for spectrum while there is available spectrum. Miss detection increases the probability of collision, decreasing spectrum sharing efficiency. On the other hand, increasing T_d could also increase the spectrum sharing efficiency. Meanwhile, the delay for accessing channels could also increase when $M > N$ in this case. The performance for slotted case has been analyzed in [8].

5. EXPERIMENTAL RESULTS

Two experiments have been designed and conducted to validate the spectrum analyzer and the whole system, including flexible physical layer, spectrum analyzer and channel assignment protocol. Test equipments are NI USRP RIO 2953R and NI LabVIEW CSDS. The center frequency is 2.4 GHz for all experiments.

5.1. Experimental Results of Spectrum Analyzer

The selection of threshold should minimize the probability of false alarm and miss detection. The test is over the air through antennas. Tx and Rx ports in the same USRP are run as a SU pair for the test. The signal power is maximized in this case. PRBG 1 is chosen as an example. False alarm ratio is defined as the ratio of the number of false alarms to the total number of tests. Similarly, miss detection ratio is defined as the ratio of the number of miss detections to the total number of tests. When the test time $t \to \infty$, false alarm rate $\to P_F$, and miss detection rate $\to P_M$.

In Figure 8, false alarm rate is tested for the signal of noise, signal from adjacent side lobe and IQ imbalance signal as a function of threshold-to-noise ratio (TNR). The false alarm rate for noise is tested when Tx is turned off. The false alarm rate for side lobe is tested on PRBG 2 when PRBG 1 is turned on for data transmission. The false alarm rate for IQ imbalance signal is

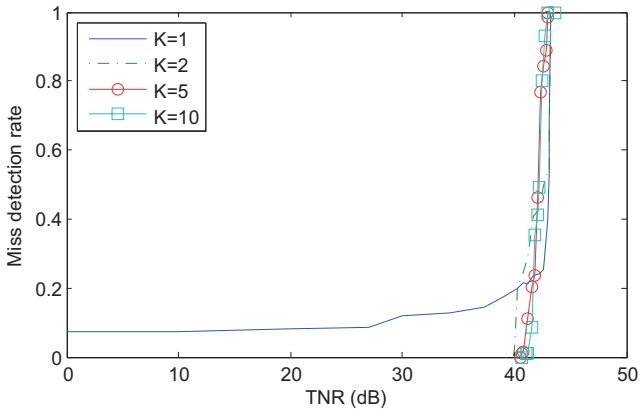

Figure 10: The miss detection rate as a function of TNR. SNR= 42 dB. $K = 1, 2, 5, 10$.

tested on PRBG 10 when the data signal is transmitted on PRBG 1. PRBG 10 and PRBG 1 are symmetric with respect to the DC. We choose the USRP with the worst IQ imbalance performance for test to highlight the effects of IQ imbalance on spectrum sensing. The power of IQ imbalance signal is about 22.5 dB higher than the noise, while the side lobe power is about 12 dB higher than the noise. From the test result, the threshold should be several dB higher than the IQ signal imbalance to make sure the false alarm rate is close to 0.

In Figure 9, we measure the false alarm rate of IQ imbalance signal as a function of TNR for different K. Again, as shown in Figure 5, K is the number of FFT symbols to calculate moving average across time for spectrum sensing. The test results show that the false alarm rate decreases quickly from 1 to 0 when threshold is about 1.5 dB higher than the IQ imbalance signal. When $K = 1$, the signal to the spectrum analyzer occasionally comes from UL subframe, where there is no signal currently. It explains the false alarm curve for $K = 1$ is less than 1 even for

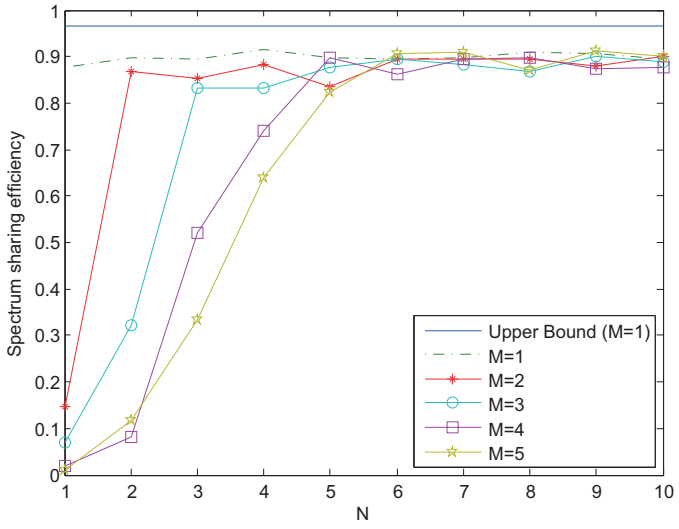

Figure 11: Spectrum sharing efficiency as a function of the number of available channels N. Full data rate, MCS $= 13$ (16QAM and coding rate 0.48). $T_s = 0.2s$. T_d and T_b have uniform distribution. $T_d \sim U(2s, 7s)$ and $T_b \sim U(0, 0.2s)$. $M = 1, 2, 3, 4, 5$. SNR=42 dB.

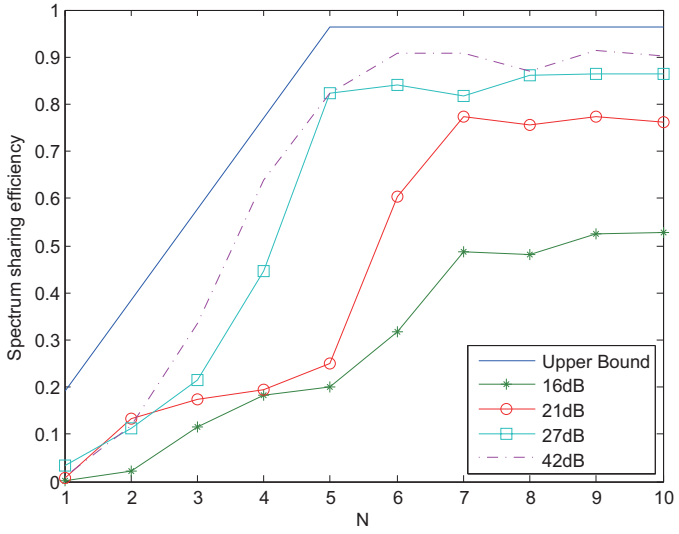

Figure 12: Spectrum sharing efficiency as a function of the number of available channels N for SNR=16, 21, 27, 42 dB. Full data rate, $M = 5$ and MCS $= 13$ (16QAM and coding rate 0.48). $T_s = 0.2s$. T_d and T_b have uniform distribution. $T_d \sim U(2s, 7s)$ and $T_b \sim U(0, 0.2s)$.

small threshold.

In Figure 10, the signal miss detection rate is tested as a function of TNR for different K. When $K = 1$, the miss detection is always larger than 0, because of the empty UL subframe. When $K \geq 2$, the miss detection is zero when threshold is about 2 dB smaller than the signal power.

In summary, $K \geq 2$ is required. To avoid false alarm, threshold should be at least 1 dB higher than the maximum of noise power, side lobe power and power of IQ imbalance signal. The threshold should be at least 2 dB smaller than the signal power to avoid miss detection. IQ imbalance comes from hardware, and it varies for different USRPs. If the channel with IQ imbalance signal is considered as not available, spectrum opportunity is wasted. On the other hand, if the channel with IQ imbalance signal is considered as available, IQ imbalance signal could interfere with the data signal. The IQ imbalance would degrade the system performance, which will be shown in the system tests.

$K = 2$ corresponds to 2 ms of spectrum sensing. In practice, the radio needs 200 ms of spectrum sensing, part of which is for transition between sensing and data transmission. Finally, we select $T_s = 200$ ms and $K = 10$. Threshold is chosen to be 5 dB higher than the maximum side lobe power.

5.2. Experimental Results of Spectrum Sharing Efficiency

For the purpose of demonstration, all the USRPs for Transmitting are located closely to minimize the spectrum sensing error and to reduce the hidden node issue. The total number of available channels N is manually selected so that database is not necessary here. All SUs are assumed to have enough data so that they need to be active for data transmission all the time.

Figure 11 illustrated the result for spectrum sharing efficiency for high SNR (42 dB). There is gap between the upper bound and the actual measured spectrum sharing efficiency. The gap is caused by false alarm, miss detection, collision as well as transition between spectrum sensing and data transmission. The gap also exists when there is only one SU, showing that transition is the main cost. More efforts are going on to reduce the transition time. Overall, the system has better performance when $M \geq N$. When $M < N$, collisions happen more frequently.

Figure 12 shows the spectrum sharing efficiency with several SNRs. As SNR increases, the performance of spectrum sharing efficiency increases. When SNR is relatively small, such as 16 dB, the spectrum sharing efficiency is far off the upper bound. The physical layer with SNR=16 dB cannot obtain full data success rate without interference according to the tests in [15]. The tests in [15] also show that physical layer could achieve full data rate when SNR$>$ 17 dB. However, there is a gap between the spectrum sharing efficiency of SNR$=$ 21, 27 dB and SNR=42 dB, which are all higher than the requirement, SNR$>$ 17 dB. False alarm and miss detection of the spectrum analyzer could be one reason. The interference of the IQ imbalance signal also plays another significant role.

Figure 13 illustrates an example of the increase of minimum SNR required for full data rate because of the interference of IQ Imbalance signal. When the IQ imbalance signal is 9.9 dB, another 10 dB Transmission power is required for full data success rate. When the spectrum analyzer treats the IQ imbalance as other SUs' signal, the spectrum opportunity could be wasted. When the IQ imbalance is considered as noise by the spectrum analyzer, it could interfere with other SUs' data signal.

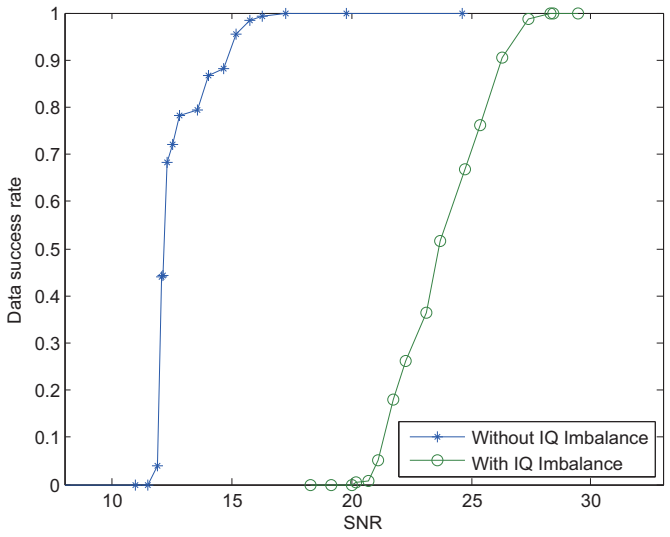

Figure 13: Examples of data success rate with and without IQ Imbalance signal as interference. The IQ Imbalance signal is 9.9 dB higher than noise while the SNR of the signal that causes the IQ imbalance is about 42dB. PRBG 1 is for data transmission. The signal that causes IQ imbalance is transmitted on PRBG 10 so that the IQ imbalance is on PRBG 1. MCS = 13 (16QAM and coding rate 0.48).

6. CONCLUSION AND ONGOING WORK

We have developed the system architecture for the distributed spectrum sharing system. The requirements for the four components of the system, i.e., database, wideband spectrum sensing, channel assignment protocol and flexible physical layer, are discussed separately. A flexible physical layer, a spectrum analyzer and a channel assignment protocol are developed based on the NI LTE AF. We introduce the details of the design, and conduct experiments to validate the architecture of the wideband spectrum sharing radio. Tests showed that the radio is robust to out-of-band interference, and the radios can share the spectrum efficiently when the number of channels is larger than or equal to the number of users and when the SNR is high enough to overcome the interference of IQ imbalance.

More work is going on to improve the synchronization performance of the physical layer, to calibrate the IQ imbalance of specific USRPs, and to improve the performance of transition between spectrum sensing and data transmission. The whole system will also be optimized and tested in a larger network with dozens of radio nodes. We could design and implement a database, and merge it into the system. Finally, the advantages of our spectrum sharing radios could combine with those of other radios to achieve better performance.

ACKNOWLEDGMENT

This work has been partially supported by NSF Grant CCF11-17365. We thank Jörg Hofrichter, Amal Ekbal, Markus Unger and Ian Wong from National Instruments, who provided insight and expertise on the LTE Application Framework.

REFERENCES

[1] Cisco Systems Inc., "Cisco visual networking index: Global mobile data traffic forecast update, 2015-2020," Feb. 2016. [Online]. Available: http://www.cisco.com/c/en/us/solutions/collateral/service-provider/visual-networking-index-vni/mobile-white-paper-c11-520862.pdf

[2] President's Council of Advisors on Science and Technology (P-CAST), "Realizing the full potential of government-held spectrum to spur economic growth," White House Office of Science and Technology Policy (OSTP), Report to the president, July 2012.

[3] O. El Ayach, S. Rajagopal, S. Abu-Surra, Z. Pi, and R. W. Heath, "Spatially sparse precoding in millimeter wave MIMO systems," *IEEE trans. Wireless Commun.*, vol. 13, no. 3, pp. 1499–1513, 2014.

[4] Q. Zhao and B. Sadler, "A survey of dynamic spectrum access," *IEEE Signal Processing Mag.*, vol. 24, pp. 79–89, May 2007.

[5] Z. Sun and J. N. Laneman, "Performance metrics, sampling schemes, and detection algorithms for wideband spectrum sensing," *IEEE Trans. Signal Process.*, vol. 62, no. 19, pp. 5107–5118, Oct. 2014.

[6] Nantional Spectrum Consortium, "About NSC," Nov. 2015. [Online]. Available: http://www.nationalspectrumconsortium.org/#about

[7] FCC, "Report and order and second further notice of proposed rulemaking," April 2015. [Online]. Available: https://apps.fcc.gov/edocs_public/attachmatch/FCC-15-47A1.pdf

[8] M. Cai and J. N. Laneman, "Database-aided distributed channel assignment in spectrum sharing," in *Proc. Allerton Conf. Communications, Control, and Computing*, Monticello, IL, Oct. 2015, pp. 1158–1165.

[9] F. Paisana, J. P. Miranda, N. Marchett, and L. A. DaSilva, "Database-aided sensing for radar bands," in *IEEE Dynamic Spectrum Access Network (DySPAN)*, Apr. 2014, pp. 1–6.

[10] H. Wang, G. Noh, D. Kim, S. Kim, and D. Hong, "Advanced sensing techniques of energy detection in cognitive radios," *Journal of Communications and Networks*, vol. 12, no. 1, Feb. 2010.

[11] X. Chen and J. Huang, "Database-assisted distributed spectrum sharing," *IEEE J. Sel. Areas Commun.*, vol. 31, pp. 2349–2361, Nov. 2013.

[12] L. Ma, X. Han, and C. Shen, "Dynamic open spectrum sharing MAC protocol for wireless ad hoc networks," in *IEEE DySPAN 2005*, Nov. 2005, pp. 203–213.

[13] P. Bahl, R. Chandra, and J. Dunagan, "SSCH: Slotted seeded channel hopping for capacity improvement in IEEE 802.11 Ad-Hoc wireless networks," in *MobiCom' 04*, 2004.

[14] A. Nasipuri, J. Zhuang, and S. R. Das, "A multichannel CSMA MAC protocol for multihop wireless networks," in *IEEE Wireless Communications and Networking Conf. (WCNC)*, 1999, pp. 1402–1406.

[15] M. Cai and J. N. Laneman, "Database- and sensing-based distributed spectrum sharing: Flexible physical-layer prototyping," in *Proc. Asilomar Conf. Signals, Systems, and Computers*, Monterey, CA, Nov. 2015.

[16] National Instrument, "LabVIEW communications system design suite," Feb. 2016. [Online]. Available: http://www.ni.com/labview-communications/

[17] M. Cai, "Design and implementation of a distributed spectrum access system," Master's thesis, University of Notre Dame, 2014.

[18] N. Theis, R. Thomas, and L. DaSilva, "Rendezvous for cognitive radios," *IEEE Trans. Mobile Computing*, vol. 10, no. 2, pp. 216–227, Feb. 2011.

[19] K. Bian and J. Park, "Asynchronous channel hopping for establishing rendezvous in cognitive radio networks," in *Proc. IEEE INFOCOM*, Shanghai, Apr. 2011.

[20] R. Gandhi, C. Wang, and C. Hu, "Fast rendezvous for multiple clients for cognitive radios using coordinated channel hopping," in *IEEE Commun. Soc. Conf. Sensor, Mesh and Ad Hoc Communications and Networks (SECON)*, June 2012.

[21] National Instrument, "NI LabVIEW Communications LTE application framework white paper," May. 2015. [Online]. Available: http://www.ni.com/white-paper/52524/en/

[22] 3rd Generation Partnership Project, "TS36.211: Evolved Universal Terrestrial Radio Access (E-UTRA); Physical Channels and Modulation (Release 10), V10.7.0," Apr. 2013.

[23] M. Mailand, R. Richter, and H.-J. Jentschel, "IQ-imbalance and its compensation for non-ideal analog receivers comprising frequency-selective components," *Advances in Radio Science*, vol. 4, no. 9, pp. 189–195, 2006.